

# DEGRADATION MECHANISMS OF MILITARY COATING SYSTEMS

L. T. Keene, G. P. Halada<sup>1</sup>, C. R. Clayton<sup>1</sup>, W.E. Kosik<sup>2</sup>, and S.H. McKnight<sup>2\*</sup>

<sup>1</sup> Dept. of Materials Science and Engineering, SUNY Stony Brook, Stony Brook, NY 11794

<sup>2</sup>Army Research Laboratory, Weapons and Materials Research Directorate  
Aberdeen Proving Ground, MD 21005 (\*Corresponding Author)

## Abstract

This work describes the development and application of specialized characterization techniques used to study the environmental degradation mechanisms of organic coating systems employed by the United States Department of Defense (DOD). Traditional methods for studying automotive and architectural coatings cannot easily probe the structural and chemical changes associated with the unique formulations used by DOD. Modified methods were developed to permit the use of Fourier Transform Infrared Spectroscopy (FTIR), Raman Spectroscopy, X-ray Photoelectron Spectroscopy (XPS), Scanning Electron Microscopy/Energy Dispersive Spectroscopy (SEM/EDS). Additionally a new method to expose coating materials through their thickness based on ultra-fast laser ablation is introduced. Four discrete coating systems subjected to established weathering protocols were studied to identify and quantify degradation mechanisms. Complementary degradation mechanisms that occur in these multi-component coating systems have been determined for the first time. The results will guide the development of more durable military coatings systems and significantly augment traditional performance assessments of coatings durability.

## 1. Introduction

**1.1 Motivation:** Polymer coating systems are applied to military assets for a variety of reasons. In addition to aesthetic appearance, the coating system must provide passive countermeasures to satisfy multiple demanding military mission requirements. Protection of military assets from environmental degradation, including corrosion is a very important contribution of the coating system. Often, the rate controlling parameter for the corrosion of military aircraft alloys is the degradation time of the protective coating system.

A military coating “system” typically consists of an inorganic pretreatment, an epoxy primer, and polyurethane topcoat (Figure 1). The goal of the surface pretreatment is to provide enhanced corrosion resistance and promote adhesion with the subsequent organic coatings. Epoxy primers are cured with polyamides or polyamines and formulated with corrosion inhibiting



**Figure 1:** Schematic of coating system constituents.

pigments for maximum performance. The primers are designed to wet the surface, provide adhesion, and inhibit corrosion. A high-solids polyurethane (PUR) topcoat is applied to the primed surface for further environmental protection and to provide desired optical properties. The coating system as a whole acts to meet protection and mission requirements. While these components are also typical of many industrial and architectural coatings systems, the specific formulation and application procedures are often significantly different from systems used for commercial applications.

A number of difficult and complex issues are associated with the degradation of military coating systems. Unlike automotive coatings, the basic PUR camouflage topcoats applied to Army and Marine Corps tactical vehicles and aircraft are highly pigmented and posses low gloss ( $60^\circ \leq 1.0$  &  $85^\circ \leq 3.5$ ) (e.g., MIL-P-46168). Topcoats for fixed-wing aircraft used by the military are based on similar PURs formulated to exhibit higher gloss. This paper reports on degradation of both ground vehicle and aircraft coatings used for military applications.

The structure and properties of military coating systems will depend on the system that is selected. The chemistry and behavior of water reducible PUR coatings are expected to differ from solvent-based coating systems. Indeed, it has been shown that the glass transition temperature and viscoelastic properties of the water reducible CARC are much different than the solvent-based MIL-C-46168 coating, e.g.,  $T_{gWR}=39.7^\circ C$  and  $T_{gSOL}=91.6^\circ C$  (Eng, et al. 2003). One should expect that these differences in structure and properties will have an effect on critical degradation properties including moisture transport, UV resistance, hydrolysis resistance, and mechanical properties.

An understanding of the degradation behavior of these coating systems is very important and could lead to

<b>Report Documentation Page</b>			<i>Form Approved OMB No. 0704-0188</i>		
<p>Public reporting burden for the collection of information is estimated to average 1 hour per response, including the time for reviewing instructions, searching existing data sources, gathering and maintaining the data needed, and completing and reviewing the collection of information. Send comments regarding this burden estimate or any other aspect of this collection of information, including suggestions for reducing this burden, to Washington Headquarters Services, Directorate for Information Operations and Reports, 1215 Jefferson Davis Highway, Suite 1204, Arlington VA 22202-4302. Respondents should be aware that notwithstanding any other provision of law, no person shall be subject to a penalty for failing to comply with a collection of information if it does not display a currently valid OMB control number.</p>					
1. REPORT DATE <b>00 DEC 2004</b>	2. REPORT TYPE <b>N/A</b>	3. DATES COVERED <b>-</b>			
4. TITLE AND SUBTITLE  <b>Degradation Mechanisms Of Military Coating Systems</b>			5a. CONTRACT NUMBER		
			5b. GRANT NUMBER		
			5c. PROGRAM ELEMENT NUMBER		
6. AUTHOR(S)			5d. PROJECT NUMBER		
			5e. TASK NUMBER		
			5f. WORK UNIT NUMBER		
7. PERFORMING ORGANIZATION NAME(S) AND ADDRESS(ES) <b>Dept. of Materials Science and Engineering, SUNY Stony Brook, Stony Brook, NY 11794; Army Research Laboratory, Weapons and Materials Research Directorate Aberdeen Proving Ground, MD 21005</b>			8. PERFORMING ORGANIZATION REPORT NUMBER		
9. SPONSORING/MONITORING AGENCY NAME(S) AND ADDRESS(ES)			10. SPONSOR/MONITOR'S ACRONYM(S)		
			11. SPONSOR/MONITOR'S REPORT NUMBER(S)		
12. DISTRIBUTION/AVAILABILITY STATEMENT <b>Approved for public release, distribution unlimited</b>					
13. SUPPLEMENTARY NOTES <b>See also ADM001736, Proceedings for the Army Science Conference (24th) Held on 29 November - 2 December 2005 in Orlando, Florida. , The original document contains color images.</b>					
14. ABSTRACT					
15. SUBJECT TERMS					
16. SECURITY CLASSIFICATION OF:			17. LIMITATION OF ABSTRACT <b>UU</b>	18. NUMBER OF PAGES <b>8</b>	19a. NAME OF RESPONSIBLE PERSON
a. REPORT <b>unclassified</b>	b. ABSTRACT <b>unclassified</b>	c. THIS PAGE <b>unclassified</b>			

reduced painting costs as well as reduce the environmental impact of painting operations. DOD painting and depainting operations are very costly as well as a significant source of hazardous waste. For example, the annual cost of corrosion in the US and DOD has been estimated at \$250B and \$10B respectively, and the degradation time of the protective coating is one rate controlling parameter. An understanding of degradation mechanisms can lead to the development of more durable systems and reduce life-cycle costs.

**1.2 Background:** Degradation mechanisms of military coatings systems are not well understood due to the unique materials, service conditions and performance requirements of these systems as compared to the commercial products used in applications such as automotive and architectural finishes. Degradation of coatings due to environmental exposure is an intensely studied topic. Most work has examined model or commercial systems primarily for automotive applications. Many efforts have focused on relating accelerated lab tests to actual service conditions. Coating appearance is evaluated by observing changes in color and gloss after exposure to various weathering conditions (outdoor and accelerated laboratory weathering) and correlating these performance metrics to corresponding changes in the chemical and physical properties of the coating are related to these exposures. This is a difficult task due to the unpredictable nature of weather and the inability to artificially duplicate exact environmental conditions. Also, the response of the coating system to the environment is complicated and depends on resin type, pigment-resin, primer-topcoat, and primer-substrate interactions. Each element must be addressed to fully understand the degradation mechanisms of the coating system as a whole. Nevertheless, much useful information has been obtained that serves to both screen coatings durability and indicate useful service life.

Failure of military coatings due to environmental degradation is more complex. The specific failure criteria will vary depending on the function of the coating. For example, the coating system may still provide adequate protection of the substrate from corrosion, but have deteriorated appearance properties (e.g., fading, color change, gloss change, chipping, peeling, etc.).

Exposure to UV radiation and moisture can chemically change the resin system in the topcoat (12,13). The response of the coating is dependent on both the UV absorbance of the material and the intensity of the exposing light. UV radiation (290–400) causes polymer chain scission and oxidation. The chemical changes lead to physical and mechanical property deterioration. Chalking of the surface can occur, and discoloration of

the resin itself is often observed. The degraded polymer can be embrittled and the mechanical properties of the “composite” pigmented coating deteriorate, which facilitates chipping, cracking, and loss of adhesion. Moisture is absorbed into the resin and can attack both the resin and the pigment-resin interface resulting in chalking. Moisture induced chemical changes including hydrolysis can be a major degradation factor in PURs.

The effect of UV weathering on polyurethane coatings has been documented previously. Published research on the degradation of a polyester polyol/aliphatic isocyanate clear coats has indicated that exposure caused general photo-oxidation as well as chain scission of the urethane cross-links (Wilhelm, et al. 1997; Irusta, et al. 1999). These studies of model poly(ester-urethane) polymer systems have provided valuable insight into urethane linkage degradation and its reactivity in the absence of other reactive sites or polyester bi-product influence. This work will be utilized in interpreting the observations made in our fully pigmented military coating systems. The focus of this work will examine four polyester-polyurethane based top-coats. Spectroscopic analysis (FTIR, ATR-FTIR, and XPS) of the coating systems A and B topcoat will examine chemical degradation due to UV exposure. These methods were able to identify quantify the temporal and special changes in coating chemistry and properties.

## 2. Approach

**2.1 Materials:** Four coating systems were studied. Two systems used on Army assets and two systems used in Navy aviation applications. The complete composition of the coatings was not disclosed by the suppliers, but the major ingredients can be described generically.

**Coating A:** (MIL-C-46168) Army CARC system.

i) Top Coat: Solvent based aliphatic polyester with siliceous extenders

ii) Primer: MIL-P- 53022 Solvent Based Epoxy

**Coating B:** (MIL-DTL-64159) Low-VOC Army CARC

i) Top Coat: Water Dispersible CARC Polyurethane with polymeric bead extenders. Aliphatic PUR dispersion and modified isocyanates

ii) Primer: MIL-P- 53030 water Based Epoxy

**Coating C:** (MIL-C-85285), Navy Aviation System

i) Top Coat: Solvent based Polyurethane Aliphatic isocyanates and polyester polyols

ii) Primer: MIL-P- 23377Solvent Based Epoxy

**Coating D:** Navy Zero-VOC developmental coating

i) Top Coat: Water based aliphatic PUR.

ii) Primer: MIL-P- 85582 water Based Epoxy

While a thorough study has been completed for these coatings systems, this report will focus on the environmentally induced changes in the topcoats. All four topcoats incorporate polymer binders comprised of

two-part aliphatic poly(ester-urethane) (either solvent or water based, depending on the coating system). The poly(ester-urethane) binder is formed at the time of application and is generated via reaction between a hydroxide group carried by a polyol and an isocyanate group (Wicks, et al. 1999) (Figure 2). All coating systems being evaluated have major constituents based on isocyanurate or biuret form of hexamethylene diisocyanate (HDI) (Figure 3). Coatings "A" and "C" employ organic solvents, and coatings "B" and "D" have sharply reduced or otherwise completely eliminated these organics in favor of a water-based reduction.

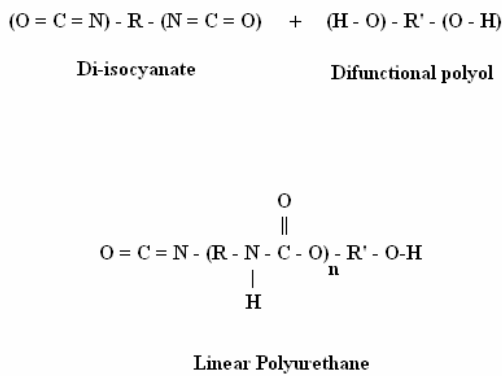


**Figure 2:** Ideal polyurethane chemistry in two part coatings. (Potential side reactions not included for simplicity.)

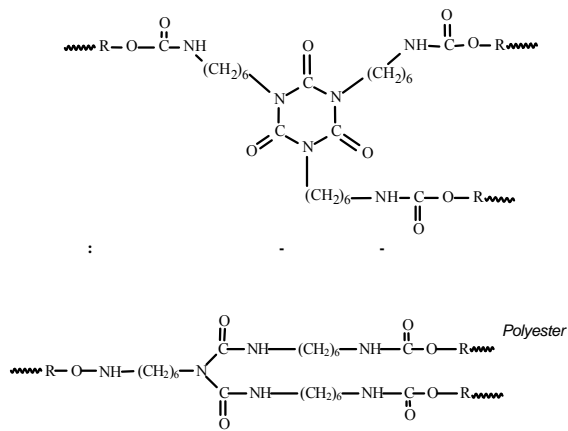


**Figure 3:** HDI based polyurethanes. A) HDI isocyanurate. B) HDI biuret.

**2.3: Weathering:** Coated panels were exposed to a variety of weathering exposures. These exposures included both accelerated laboratory weathering protocols (QUV chambers) and true environmental aging at Arizona and Florida test sites. Panels were periodically removed from the weathering environments and examined using a variety of analytical techniques to determine the mechanisms of degradation. A parallel

study (not reported here) evaluated the performance parameters of the coating after weathering exposures (Kosik, et al., SERDP PP-1133 Final Report 2003).

**2.3: Experimental Methods:** The high pigment loading of military coatings significantly hinders the routine application of traditional coatings analysis techniques. The optical opacity, thickness, roughness, and electrical charging of these coating systems seriously complicate any analysis routine. Methods can be developed to address these problems. First, micro ATR-FTIR spectroscopy employing a diamond internal reflection element was used to characterize the surface chemistry of the coatings. Careful preparation of sample cross-sections using microtomy methods enabled through-thickness measurements using the high brightness infrared source at the National Synchrotron Light Source (NSLS) at Brookhaven National Laboratory. The higher intensity radiation permitted high resolution transmission FTIR measurements to augment optical and electron microscopy evaluations. Specific descriptions of measurement techniques are described below.

**Electron Microscopy and Energy Dispersive Spectroscopy:** Cross-sections of coatings were prepared by immersing samples in liquid N<sub>2</sub>, resulting in the intact debonding of the coating samples from the metal substrates. The samples were then embedded in histological wax embedding compound (Paraplast<sup>TM</sup> X-TRA Tissue Embedding Medium) and allowed to solidify. Samples were microtomed to a thickness of 10  $\mu\text{m}$  using a Leica<sup>TM</sup> RM2125 microtome equipped with disposable steel blades and mounted on vacuum-compatible copper tape. Prior to insertion in the SEM, samples were exposed to 10 seconds gold sputtering to facilitate charge compensation. SEM images as well as EDS spectra were collected for baseline (unexposed) samples for both coating systems.

**Micro-ATR-FTIR:** Measurements were performed using a Nicolet Magna Spectrometer with attached NIC Plan microscope outfitted with a diamond tip ATR attachment. The choice of internal reflection element was critical to the successful measurement of IR spectra. The diamond tip ensures good optical contact to the sample contact resulting in better spectra quality for these very rough and hard coating specimens.

**X-ray photoelectron spectroscopy (XPS)** A Kratos X-ray photoelectron spectroscopy system was used to characterize the near surface composition of the as-deposited and aged coating systems. All spectra were taken at a  $2 \times 10^{-9}$  torr vacuum environment or better.

**Cross-sectioning and Transmission FTIR:** Effective mechanical cross-sectioning techniques were able to produce coatings cross sections that have been successfully studied by SEM and micro-FTIR. The

minimum achievable thickness for the cross-sections was 3  $\mu\text{m}$  for systems B, C and D. FTIR transmission measurements of these samples resulted in sufficient signal-to-noise for proper peak separation and intensity determination. Unfortunately, System A exhibits insufficient plasticity for effective cross sectioning and could not be studied in this manner.

After sectioning the embedded samples are placed on 2 mm BaF<sub>1</sub> or KBr transmission windows. FTIR spectroscopy was conducted in transmission mode using microscope aperture dimensions of 10  $\mu\text{m} \times 70 \mu\text{m}$  (height x width). The aperture was raster-scanned in a rectangular pattern across the cross-section from the primer/topcoat interface to the topcoat surface in steps of 4 in the horizontal (zero overlap) and a 50% (5  $\mu\text{m}$ ) overlap in the vertical direction (Figure 4). Spectra were collected using 256 averaging scans at 4  $\text{cm}^{-1}$  resolution.

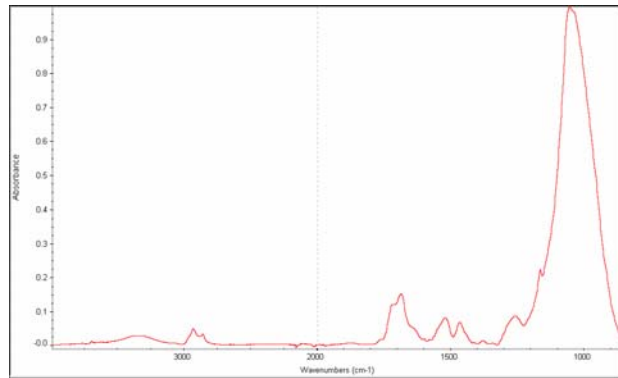


Figure 4: ATR FTIR spectra of Coating A

**Laser Ablation:** Laser ablation provided a means to depth profile the coatings. The method has not been used in this manner before, and results are still considered preliminary. A Ti:Sapphire amplified laser with 740 nm wavelength, 30 femtosecond pulse duration and approx. 30  $\mu\text{m}$  spot size was used to create a series of ablated windows on the coating surface. By choosing laser power and scan speed a series of windows were ablated in coating system C at various combinations of power and scan speed generating 3 columns of progressively deeper windows in the topcoat. The columns were created using laser powers of 167, 73 and 35 micro Joules respectively. All three columns consisted of 5 ablation windows, each created with scan speeds ranging from 2000 to 10,000 microns. Depth and morphology of each window was determined by scanning confocal profilometry.

### 3. Results and Discussion

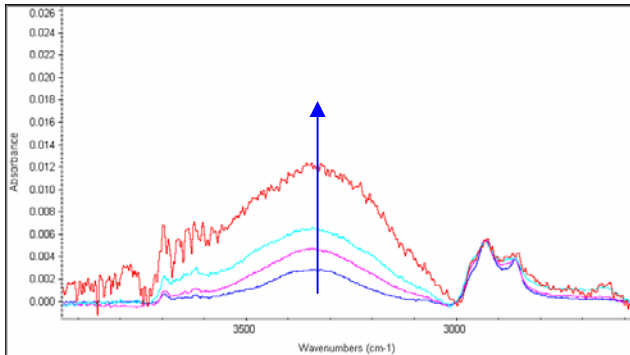
While thorough study of all coating systems has been conducted, it is not possible to review and discuss each system in detail in this paper. Specific findings can be discussed and the utility of the tools that have been

developed can be illustrated. The surface FTIR measurements of the coatings after aging can clearly point to the photodegradation mechanisms and their kinetics. Figure 4 shows the FTIR-ATR spectra of Coating A. A few spectral features are important to note. The PUR found in Topcoat A is formulated with an HDI biuret reacted with a saturated polyester polyol resin and uses siliceous based extenders. The broad band above 3000  $\text{cm}^{-1}$  can be attributed to OH species and primary/secondary amine functionalities. The bands between 2859  $\text{cm}^{-1}$  and 2935  $\text{cm}^{-1}$  arise from asymmetric and symmetric aliphatic CH<sub>2</sub> stretching vibrations. Several carbonyl (C=O) species from the PUR polymer are noted by bands near 1650–1780  $\text{cm}^{-1}$ . The amide II band found between 1510 and 1550  $\text{cm}^{-1}$  is also present as expected. The amide II is important since degradation can be related to the reduction in intensity of this band (Yang, et al. 2002). The aliphatic backbone of the PUR results in a well-defined peak at 1466  $\text{cm}^{-1}$ . The dominant band from 900 to 1250  $\text{cm}^{-1}$  results from the presence of silica in the coating. Also, no un-reacted isocyanate was detected as shown by the absence of any isocyanate band usually located near 2150  $\text{cm}^{-1}$ . This indicates a well cured system. These values and interpretations are consistent with previously researched literature on aliphatic coating systems and band assignments for coatings C and D are noted in Table 1 (Yang, et al. 2002; Wilhelm, et al. 1997).

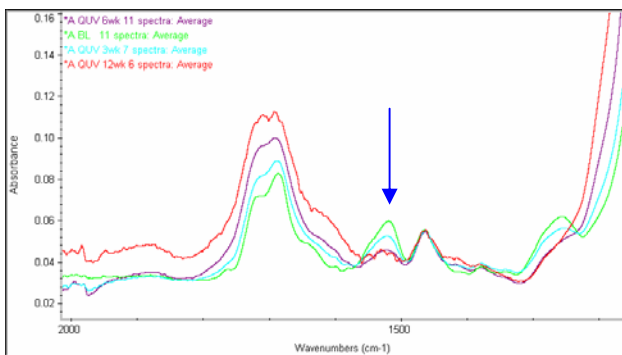
TABLE 1 Band assignments for spectral features found in Coatings C and D. (Coatings A and B share many band assignments.)

Frequency ( $\text{cm}^{-1}$ )	Relative Intensity	Main assignments
3364(c), 3340(d)	M	$\nu$ (OH) H-bonded
2937(c), 2929(d)	S	$\nu_{\text{as}}$ (CH <sub>2</sub> ) in HDI
2863(c/d)	M	$\nu_{\text{sym}}$ (CH <sub>3</sub> ) in HDI
1767(d)	M	
1725(c), 1719(d)	Vs	$\nu$ (C=O) in ester
1685(c), 1692(d)	Vs	$\nu$ (C=O) in urethane
1523(c), 1529(d)	S	$\nu$ (C-N) + $\delta$ (N-H) (amide II)
1464(c), 1463(d)	S	$\delta$ (CH <sub>2</sub> )
1430(c), 1426(d)	w, sh	$\delta$ (CH <sub>3</sub> )
1376(c/d)	M	$\delta$ (CH <sub>3</sub> )
1234(c), 1237(d)	s, sh	$\nu$ (C=O) + $\nu$ (O-CH <sub>2</sub> ) ester
1171(c), 1179(d)	s, sh	$\nu$ (C-O-C) ester
1136(c), 1140(d)	s, sh	$\nu$ (C=O) + $\nu$ (O-CH <sub>2</sub> )
1068(c), 1075(d)	Vs	$\nu_{\text{as}}$ (O-Si-O)
1017	s, sh	$\nu$ (Si-O-NBO)

Figures 5a and 5b show changes IR spectra of Coating A as a function of QUV artificial weathering exposure. The dominant UV degradation in the presence of oxygen is the oxidation of the urethane linkage. This can be seen by the reduction in intensity of the amide II band and the increase in COOH peaks. The CH<sub>2</sub> bands associated with the aliphatic polymer backbone remain relatively constant indicating little if any degradation in this region of the polymer. This is consistent with



(a)



(b)

**Figure 5:** Micro-ATR-FTIR spectra of Coating A after aging.

literature descriptions. Also the degradation mode seen in QUV samples agrees well with environmental aging in Florida and Arizona. At the same time the relative intensity of the silica peak grew relative to the polymer species indicating an increased contribution of silica to the surface chemistry and decreased polymer content at the surface. This is consistent with related studies described in the literature (Hare 2001).

The increased resistance to photodegradation of Coating B is noteworthy. Figure 6 shows the spectra of Coating B after QUV exposure. This water reducible system is more highly indexed (greater NCO:OH ratios) than the solvent based materials which may account for the differences. Also, the starting materials are different that may also contribute to the enhanced durability. For similar exposures there is very little degradation of the polymer as indicated by the very strong amide II band. This corresponds well to the increased resistance to color change and fading in these systems when compared to system A (Kosik, et al., SERDP PP-1133 Final Report 2003).

The observed changes in polymer surface chemistry of Coating C determined using infrared spectroscopy methods were similar to those seen in Coating A. The decreased amide II intensity relative to other polymer bands is evident (Figure 7). The depth of degradation in

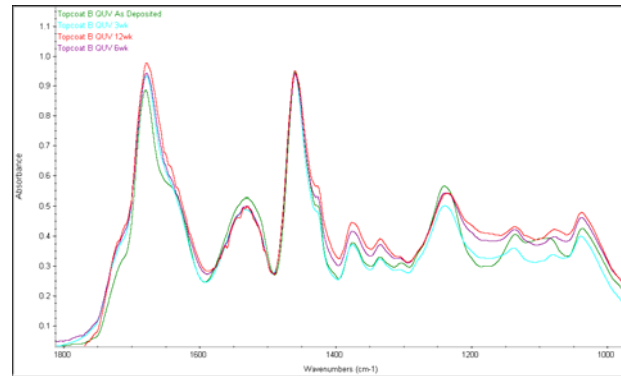


**Figure 6:** Fingerprint region ATR spectra for Coating B with various QUV exposure durations.

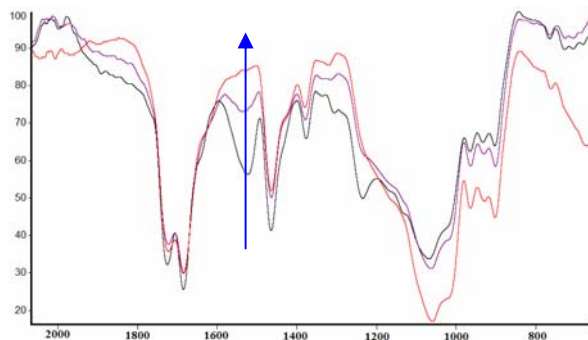


**Figure 7:** Representative FTIR spectra obtained from Coating C surface after exposure to QUV Evolution after 6, 12, and 18 weeks. Note a dramatic reduction of amide II ( $1523\text{ cm}^{-1}$ ).

Coating C was also examined. Before discussing the spectroscopy depth profiling results, it is useful to describe the complex microstructure of the coating system. A typical electron micrograph of Coating C is shown in Figure 8. The complexity of the coating system is clear. The stratified differences between topcoat and primer are evident as is the heterogeneous distribution of the prime pigments and extenders. The image in Figure 9 further demonstrates the complex microstructure as shown by the EDS elemental mapping. The complexity is important to recognize when evaluating the difficulty in sample preparation and data analysis. Cross-sections were difficult to produce and several spectra must be measured to adequately describe the polymer chemistry.

The spatial variation in coating chemistry changes after aging was evaluated using the transmission FTIR of the microtomed cross-sections. Due variation in composition and thickness, normalized band ratios are plotted. Reduction in the amide II band has been associated with the loss of urethane linkages in polyurethane coatings and, therefore, can be used to characterize the photooxidation process. The intensity of this band is normalized by the hard-segment urethane carbonyl band at 1685 wavenumbers (this band has been observed to increase as a function of UV exposure and, hence, as the

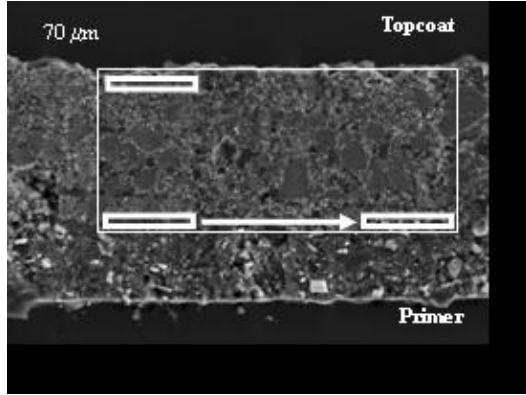


**Figure 8:** SEM micrograph of a primer-topcoat cross section for system C. The smaller rectangular boxes indicate the window size for FTIR analysis.

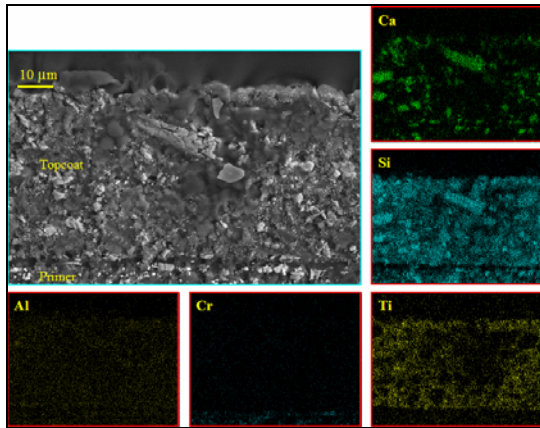


**Figure 9:** SEM image of coating system C topcoat and associated elemental maps from EDS.

normalizing denominator can be used to amplify the response of the ratio to UV degradation). The ratio is constructed using peak heights and not peak areas. The ratios are meant to discern the depth of degradation, and should not be viewed as quantitative due to the complex reactions and byproducts that produce new bands in the IR spectra. A common photodegradation model results in a net increase of carbonyl activity and urethane end groups (as seen from the reduction of amide II and growth of an absorption band at  $1607\text{ cm}^{-1}$ , as well as the development of a carbonyl shoulder at  $1755\text{ cm}^{-1}$  due to acetylurethane photoproduct), an effect that can be expected to amplify the peak height ratio calculation. Thus the data presented in Figure 10 shows a comparison between baseline (unexposed) and maximum exposure samples. This important data shows for Coating C that the degradation progresses well into the thickness of the coating.

The IR data for the coatings can be complimented by XPS analysis. XPS is more surface sensitive and can be used to probe the evolving atomic composition of the

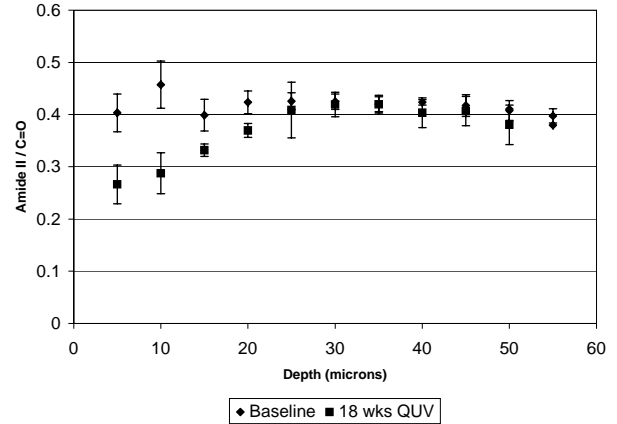


**Figure 10:** Normalized IR intensities vs. depth for Coating C comparing baseline and aged specimens.

aging samples. For example, composition measured by XPS for Coating C after QUV weathering are shown in Figure 11. The initial surface composition is high in carbon, oxygen and fluorine, with small contributions from inorganic extenders and pigments. The data shows an increase in O and Si and emergence of other inorganic elements. Also a rapid decrease in the F content is observed from fluorosurfactant degradation. The loss of carbon and rapid emergence of Si pigment/extender elements is characteristic of binder degradation. Similar results were obtained for the other coatings systems and environmental exposure conditions.

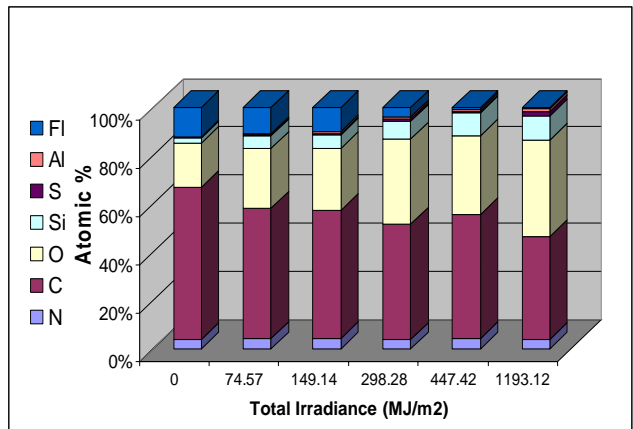


**Figure 11:** Surface composition of QUV exposed Coating C samples as determined by XPS. Increasing irradiance indicates longer exposure times.

Figure 12 shows the laser confocal microscopy images demonstrating controllable progressive ablation of a coating sample. While still in progress, the initial work has shown that controllable windows can be created at desired depths with great reproducibility. Depth and morphology of each window was determined by scanning confocal profilometry. Window depth as a

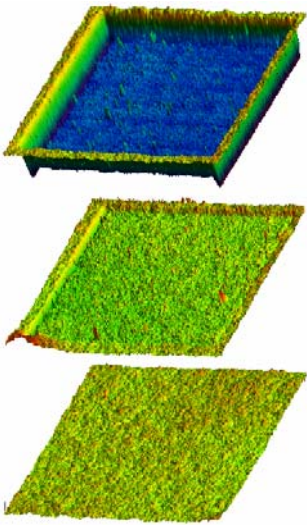


**Figure 12:** Representative laser scanning confocal microscopy images of a coating after laser ablation. The window sizes are large enough to accommodate spatially resolved surface analytical measurements including FTIR and XPS.

function of scanning speed was plotted for 3 laser powers. Process parameters were determined using-fit curve predictions. These process parameters can be used to predict depths for various coating systems. All experiments were conducted on coating systems C and D in order to provide a comparison between the cross-sectional data and the data collected via femtosecond ablation-assisted depth profiling. Analysis of the exposed window regions is ongoing.

These results point to a general mechanism for UV induced topcoat degradation. The observed mechanisms appear to be consistent for the four systems, although differences in degradation rate were observed. In previous studies of HDI-based, non-pigmented systems, loss of urethane structure was shown to proceed in the presence of UV irradiation and oxygen. FTIR spectra indicated hydroxyl formation and loss of urethane structure, but did not indicate the influence of the polyester segments on the photochemical behavior of the model aliphatic poly(ester-urethane) system. Long wavelength ( $>300$  nm) irradiation without the presence of oxygen showed no noticeable change of spectra. It has been proposed that oxidation of the C atom in alpha position to the NH urethane linkage leads to the formulation of hydroperoxides, which through a series of reactions and short-lived photoproducts results in a carboxylic acid and urethane end group. These mechanisms lead to the overall degradation of the topcoat and the associated loss of appearance. The presence of moisture and other species can accelerate or retard the rate of reaction.

Specific reasons for the observed differences in the rate of degradation of these four systems are still being

studied. However, differences in the PUR binder chemistry appear to have substantial impact. In general the PUR forms from reaction of a hydroxyl-terminated polyol with a diisocyanate as shown in Figure 1. Typical solvent based systems index the isocyanate (NCO) to (OH) at 1.1:1.0 molar equivalents. The 10% over-indexing ensures complete reaction of the polyol with the NCO. Water dispersible polyisocyanates and higher molecular weight hydroxyl-functional polyurethane dispersions are utilized in the low VOC systems and over indexing is on the order of 5.0:1.0 to account for competing reaction between NCO-water over the desired NCO-hydroxyl reaction. The NCO-water reaction results in the formation of such chemical functional groups as: urethanes, ureas, amines, and evolves carbon dioxide. The most durable coating system (Coating B) used a highly indexed water dispersible PUR binder, formed by reacting modified isocyanates with a highly engineered preformed hydroxyl functional polyurethane dispersion. The influence of the starting materials and the indexing can alter the glass transition temperature, storage modulus, film hardness and crosslink density. It appears that while the base chemistry is similar these parameters contribute to the UV resistance of the final formulation as well.

#### 4. Conclusions

This study employed methods to permit the use of Fourier Transform Infrared Spectroscopy (FTIR), X-ray Photoelectron Spectroscopy (XPS), Scanning Electron Microscopy/Energy Dispersive Spectroscopy (SEM/EDS) to study the chemistry and structure of polymer coatings. These methods were able to capture the degradation mechanisms of the PUR binders used in military topcoats. Complementary degradation mechanisms that occur in these multi-component coating systems have been determined. The resistance to UV degradation has been demonstrated to be a function of poly(ester)urethane chemistry and the pigmentation in the coating. Differences in the rate and depth of the PUR degradation were noted and could be related to coatings performance. Interestingly, the environmentally friendly coatings which meet the emerging regulations and statutes outperform the high volatile organic compound (VOC) counterparts. This important data shows that the immediate reduction in environmental impact associated with these newer products is enhanced by longer service-life. The results will guide the development of more durable military coatings systems and significantly augment traditional performance assessments of coatings durability.

## 5. Acknowledgements

This work was supported in part by the DOD SERDP Program PP-1133 under the direction of Mr. Charles Pellerin. The authors thank John Escarcega and the ARL Coatings Technology Team for their technical support and assistance. The authors also greatly acknowledge the Ultrafast Coherent Control and Spectroscopy group (Department of Physics and Astronomy SUNY Stony Brook) for the use of their laser, and the Laboratory for Experimental Mechanics Research (Department of Mechanical Engineering SUNY Stony Brook) for the use of their optical equipment.

## 6. References

- A. Eng, L., McGrath, and F. Pilgrim: Mechanisms of Military Coatings Degradation – End of Fiscal Year 2002 Report, Naval Surface Warfare Center, Carderock Division Technical Report, NSWCCD-62-TR-2003/01; December 2002.
- C.H. Hare, Protective Coatings: Fundamentals of Chemistry and Composition (The Society for Protective Coatings, Pittsburgh, 1994) 514.
- Z.W. Wicks, F.N. Jones, S.P. Pappas, Organic Coatings Science and Technology (John Wiley & Sons, New York, 1999).
- X.F. Yang, C. Vang, D.E. Tallman, G.P. Bierwagen, S.G. Croll, S. Rohlik, Polymer Degradation and Stability 74 (2001) 341.
- X.F. Yang, D.E. Tallman, G.P. Bierwagen, S.G. Croll, S. Rohlik, Polymer Degradation and Stability 77 (2002) 103.
- C. Wilhelm, J.L. Gardette, Polymer 38 (1997) 4019.
- L. Irusta, M.J. Fernandez-Berridi, Polymer Degradation and Stability 63 (1999) 113.
- C.H. Hare, Paint Film Degradation: Mechanisms and Control (The Society for Protective Coatings, Pittsburgh, 2001) 631.